Superluminal pulse propagation through one-dimensional photonic crystals with a dispersive defect

Nian-hua Liu,[1,2] Shi-Yao Zhu,[2,3] Hong Chen,[4] and Xiang Wu[4]
[1]*Department of Physics, Nanchang University, Nanchang 330047, China*
[2]*Department of Physics, Hong Kong Baptist University, Kowloon Tong, Hong Kong*
[3]*Department of Physics, Texas A&M University, College Station, Texas 77843*
[4]*Department of Physics, Tongji University, Shanghai 200092, China*
(Received 11 October 2001; published 25 March 2002)

The propagation of a pulse through one-dimensional photonic crystals that contain a dispersive and absorptive defect layer doped with two-level atoms is discussed. The dynamical evolution of the pulse inside the photonic crystal is presented. Superluminal negative group velocity (the peak appears at the exit end before it reaches the input end) is discovered. Although the group velocity is larger than c and even negative, the velocity of energy propagation never exceeds the vacuum light speed. The appearance of the superluminal advance or subluminal delay of the pulse peak inside the photonic crystal or at the exit end is due to the wave interference from Bragg reflections.

DOI: 10.1103/PhysRevE.65.046607 PACS number(s): 42.70.Qs, 41.20.Jb, 42.25.Bs, 73.40.Gk

I. INTRODUCTION

Periodic dielectric media called photonic crystals have attracted considerable attention in recent years [1]. The essential property of the photonic crystals is the band-gap structure. Multilayered medium is considered as a simple example of one-dimensional photonic crystals (1DPCs). The electromagnetic field of frequency within the gap is evanescent. Since the evanescent field is analogous to the wave function of an electron in a quantum barrier, the 1DPCs were used as an optical barrier to investigate the tunneling time [2–4]. The tunneling time of an optical pulse through the optical barrier was proved to be superluminal.

The time delay of pulse propagation through dielectric media is defined as $t_d = t_0(c/v_g - 1)$, where t_0 is the time through the same vacuum distance, and v_g is the group velocity. The group velocity, according to the definition, $v_g = d\omega(k)/dk$, is dependent on the frequency-wave number dispersion relation. The dispersion of media originates from the interaction of light with matter. There are two kinds of resonant interaction. One is that the light frequency matches a transition frequency of atoms or molecules. Around the resonant frequency the dielectric function or refractive index is frequency dependent. This kind of dispersion is usually referred to as material dispersion. The other occurs when the light wavelength matches a characteristic length of the media, for example, the size of a dielectric cell in the photonic crystals. In this case the Bragg reflection becomes strong. As a result, a stop band or forbidden gap is created. Near the band edge, the dispersion relation is significantly modified. This kind of dispersion is usually referred to as structural dispersion.

The dispersion relation $\omega(k)$ for infinite 1DPCs can be derived from Bloch's theorem [5]. For finite 1DPCs, the dispersion behavior can be described by an effective refractive index that is defined via the complex transmission coefficient [6,7], and the group velocity can be calculated from the effective refractive index. In the stop band the effective refractive index is anomalous. Therefore, the propagation of pulses in the stop band is superluminal. Near the band edge, however, the effective refractive index has a positive steep slope such that group velocity can be slowed [8,9]. Particularly, if a periodic 1DPC is perturbed by a defect layer, the slope of the effective refractive index at the defect mode frequency will become very steep, which causes a great group delay [6].

The superluminal propagation has been an interesting subject in recent years [10]. Although the superluminal phenomena were observed experimentally, the mechanism remains controversial [11]. It is generally explained as reshaping of pulses. Japha and Kurizki suggested a universal mechanism for the superluminal time delays in nondissipative media [12]. They emphasized that phase coherence played a key role in the tunneling, and demonstrated that the superluminal time delay is a result of predominantly destructive interference between accessible causal paths. In a finite 1DPC, the group velocity v_g and the energy velocity v_E are not the same [13]. It is demonstrated that they satisfy [14] $v_E = |t|^2 v_g$.

In this paper, we consider the temporal-spatial evolution of a pulse inside an 1DPC. The pulse is decomposed into an integral of all Fourier components. The behavior of individual components is determined by means of a transfer matrix method, while the temporal-spatial behavior of the pulse is calculated by integrating all Fourier components. The advantage of this way is that it can deal with the case where the constituent materials themselves are dispersive. We consider not only the case that the 1DPC is made up of nondispersive materials, but also the case that the periodic 1DPC contains a dispersive defect layer. The defect layer is doped with two-level atoms that leads to a dispersion relation of Lorentz type. The combination of the structural resonance of the multilayer geometry and the atomic resonance in the defect layer leads to a large negative group velocity.

II. TRANSFER MATRIX FORMALISM FOR PULSE PROPAGATION

In an 1DPC, the propagation of an optical pulse is governed by the wave equation

$$\frac{\partial^2}{\partial z^2}\mathbf{E}(z,t)-\frac{1}{c^2}\frac{\partial^2}{\partial t^2}\mathbf{E}(z,t)=\frac{1}{\varepsilon_0 c^2}\frac{\partial^2}{\partial t^2}\mathbf{P}(z,t), \tag{1}$$

where $\mathbf{E}(z,t)$ is the electric field and $\mathbf{P}(z,t)$ is the electric polarization. Suppose that the pulse can be expressed as an integral of its Fourier components

$$\mathbf{E}(z,t)=\int \mathbf{E}(z,\omega)e^{-i\omega t}d\omega, \tag{2}$$

and the Fourier component of the polarization $\mathbf{P}(z,\omega)=\chi(z,\omega)\mathbf{E}(z,\omega)$ under linear response approximation. The equation for the Fourier component of electric field can be written as

$$\frac{d^2}{dz^2}\mathbf{E}(z,\omega)+\frac{\omega^2}{c^2}\epsilon(z,\omega)\mathbf{E}(z,\omega)=0, \tag{3}$$

where $\epsilon(z,\omega)=1+\chi(z,\omega)$ is the dielectric function.

Our method is that we firstly solve Eq. (3) layer by layer, then integrate $\mathbf{E}(z,\omega)$ by using Eq. (2) to obtain the temporal-spatial behavior of the pulse. The integral is a coherent superposition of all Fourier components including the forward waves and backward waves with complicated relations of phases.

We consider normal propagation in z direction (layers in x-y plane). The electric field is polarized along x direction. In the jth layer the electric field $E_j(z,\omega)$ satisfies

$$\frac{d^2}{dz^2}E_j(z,\omega)+\frac{\omega^2}{c^2}n_j^2(\omega)E_j(z,\omega)=0,(z_{j-1}<z<z_j,j=1,2,\ldots,N), \tag{4}$$

where $n_j(\omega)=\sqrt{\epsilon_j(\omega)}$ is the refractive index that is a constant in the same layer for a given ω. The general solution of Eq. (4) can be expressed as

$$E_j(z,\omega)=E_{+j}(\omega)\exp\left[i\frac{\omega}{c}n_j(\omega)(z-z_{j-1})\right]+E_{-j}(\omega)\exp\left[-i\frac{\omega}{c}n_j(\omega)(z-z_{j-1})\right]. \tag{5}$$

From $\nabla\times\mathbf{E}=-(\partial/\partial t)\mathbf{B}=i\omega\mathbf{B}$ we can get the magnetic field

$$B_j(z,\omega)=\frac{n_j(\omega)}{c}\left\{E_{+j}(\omega)\exp\left[i\frac{\omega}{c}n_j(\omega)(z-z_{j-1})\right]-E_{-j}(\omega)\exp\left[-i\frac{\omega}{c}n_j(\omega)(z-z_{j-1})\right]\right\}, \tag{6}$$

which is polarized along y axis. Define

$$\psi_{1j}(z,\omega)=E_j(z,\omega), \tag{7}$$

$$\psi_{2j}(z,\omega)=icB_j(z,\omega), \tag{8}$$

such that the electric component $\psi_1(z,\omega)$ and the magnetic component $\psi_2(z,\omega)$ can be measured by the same unit. The electromagnetic field then can be expressed by a two-component wave function vector,

$$\Psi_j(z,\omega)=\begin{pmatrix}\psi_{1j}(z,\omega)\\ \psi_{2j}(z,\omega)\end{pmatrix}. \tag{9}$$

From Eqs. (5) and (6) we can obtain the transfer matrix relating $\Psi_j(z+\Delta z,\omega)$ to $\Psi_j(z,\omega)$,

$$\Psi_j(z+\Delta z,\omega)=M_j(\Delta z,\omega)\Psi_j(z,\omega), \tag{10}$$

where

$$M_j(\Delta z,\omega)=\begin{pmatrix}\cos\left[\frac{\omega}{c}n_j(\omega)\Delta z\right] & \frac{1}{n_j(\omega)}\sin\left[\frac{\omega}{c}n_j(\omega)\Delta z\right]\\ -n_j(\omega)\sin\left[\frac{\omega}{c}n_j(\omega)\Delta z\right] & \cos\left[\frac{\omega}{c}n_j(\omega)\Delta z\right]\end{pmatrix}. \tag{11}$$

Because $\psi_1(z,\omega)$ and $\psi_2(z,\omega)$ are proportional to the tangential components of the electric field and the magnetic field, respectively, they are continuous function of z across the layer interfaces. At any position z, $\Psi(z,\omega)$ connects with $\Psi(z_0,\omega)$ through a propagation matrix. For example, in the jth layer $(z_{j-1}<z<z_j)$, the field at $z=z_{j-1}+\triangle z$ is

$$\Psi(z_{j-1}+\Delta z,\omega)=Q(z_{j-1}+\triangle z,\omega)\Psi(z_0,\omega), \tag{12}$$

where the propagation matrix

$$Q(z_{j-1}+\triangle z,\omega)=M_j(\Delta z,\omega)\prod_{i=1}^{j-1}M_i(d_i,\omega). \tag{13}$$

From Eqs. (12) and (13) we can calculate the electric field and the magnetic filed at any position provided that $\Psi(z_0,\omega)=[\psi_1(z_0,\omega),\psi_2(z_0,\omega)]^T$ is known.

$\Psi(z_0,\omega)$ can be determined by matching the boundary condition. Assume the light is incident from the region of $z<0$. In this region the field is a superposition of forward field and backward field,

$$E(z,\omega)=E_i(z,\omega)e^{ikz}+E_r(z,\omega)e^{-ikz}, \tag{14}$$

where $k=\omega/c$. At the incident end we have

$$\Psi(0,\omega)=\begin{pmatrix} E_i(0,\omega)+E_r(0,\omega) \\ i[E_i(0,\omega)-E_r(0,\omega)] \end{pmatrix}. \tag{15}$$

Generally, the forward (incident) field $E_i(0,\omega)$ is given, while the backward (reflection) field $E_r(0,\omega)$ is to be solved. In order to solve $E_r(0,\omega)$, another boundary condition at the exit end$z=z_N$ should be utilized. In the region of $z>z_N$, there is only forward (transmitted) field,

$$E(z)=E_t(z,\omega)e^{ik(z-z_N)}. \tag{16}$$

Thus,

$$\Psi(z_N,\omega)=\begin{pmatrix} E_t(z_N,\omega) \\ in_S E_t(z_N,\omega) \end{pmatrix}, \tag{17}$$

where n_S is the refractive index of the substrate. Suppose that the matrix connecting the incident end and the exit end is $X_N(\omega)$, we have

$$\Psi(z_N,\omega)=X_N(\omega)\Psi(0,\omega), \tag{18}$$

where

$$X_N(\omega)=\prod_{j=1}^{N} M_j(d_j,\omega)=\begin{pmatrix} x_{11}(\omega) & x_{12}(\omega) \\ x_{21}(\omega) & x_{22}(\omega) \end{pmatrix}. \tag{19}$$

Equation (18) may be rewritten in a form of

$$\Psi(0,\omega)=X_N^{-1}(\omega)\Psi(z_N,\omega). \tag{20}$$

Because $\det M_j(d_j)=1$, we have $\det X_N(\omega)=1$ and

$$X_N^{-1}(\omega)=\begin{pmatrix} x_{22}(\omega) & -x_{12}(\omega) \\ -x_{21}(\omega) & x_{11}(\omega) \end{pmatrix}. \tag{21}$$

Substituting Eqs. (15), (17), and (21) into Eq. (20) yields

$$E_r(0,\omega)=r(\omega)E_i(0,\omega), \tag{22}$$

$$E_t(z_N,\omega)=t(\omega)E_i(0,\omega), \tag{23}$$

where $r(\omega)$ is the reflection coefficient of a monochromatic plane wave of frequency ω that can be expressed in terms of the elements of the matrix $X_N(\omega)$,

$$r(\omega)=\frac{[x_{22}(\omega)-n_S x_{11}(\omega)]-i[n_S x_{12}(\omega)+x_{21}(\omega)]}{[x_{22}(\omega)+n_S x_{11}(\omega)]-i[n_S x_{12}(\omega)-x_{21}(\omega)]}, \tag{24}$$

and $t(\omega)$ is the transmission coefficient of the monochromatic plane wave that can be written as

$$t(\omega)=\frac{2}{[x_{22}(\omega)+n_S x_{11}(\omega)]-i[n_S x_{12}(\omega)-x_{21}(\omega)]}. \tag{25}$$

Thus, we can express the electromagnetic field at $z=0$ with the incident field $E_i(\omega)$ as follows:

$$\Psi(0,\omega)=E_i(0,\omega)\begin{pmatrix} 1+r(\omega) \\ i[1-r(\omega)] \end{pmatrix}. \tag{26}$$

With $\Psi(0,\omega)$ in hand, we are able to calculate the temporal-spatial behavior of the pulse. By multiplying a time factor, $e^{-i\omega t}$, to each side of Eq. (12) and integrating all frequency components, we have

$$\begin{aligned}\psi_1(z,t)&=\int \psi_1(z,\omega)e^{-i\omega t}d\omega \\ &=\int E_i(0,\omega)\{[1+r(\omega)]Q_{11}(z,\omega) \\ &\quad +i[1-r(\omega)]Q_{12}(z,\omega)\}e^{-i\omega t}d\omega\end{aligned} \tag{27}$$

and

$$\begin{aligned}\psi_2(z,t)&=\int \psi_2(z,\omega)e^{-i\omega t}d\omega \\ &=\int E_i(0,\omega)\{[1+r(\omega)]Q_{21}(z,\omega) \\ &\quad +i[1-r(\omega)]Q_{22}(z,\omega)\}e^{-i\omega t}d\omega,\end{aligned} \tag{28}$$

where $Q_{ij}(z,\omega)$ are the elements of the propagation matrix (13). The electric displacement $D(z,t)$ can be obtained through

$$D(z,t)=\epsilon_0\psi_3(z,t)=\epsilon_0\int \epsilon(\omega)\psi_1(z,\omega)e^{-i\omega t}d\omega, \tag{29}$$

where ϵ_0 is the vacuum permittivity. The unit of $\psi_3(z,t)$ is the same as $\psi_1(z,t)$ and $\psi_2(z,t)$. Obviously, the field functions given by Eqs. (27), (28), and (29) are the coherent superposition of all frequency components including forward waves and backward waves. The waves enter the integral have complicated relations of phases.

III. NUMERICAL RESULTS AND DISCUSSION

Suppose a Gaussian pulse is incident on the surface at $z=0$. The electric field of the Gaussian pulse at the surface is expressed as

$$E_i(0,t)=E_0e^{-t^2/\tau^2}, \tag{30}$$

and its Fourier spectrum is

$$E_i(0,\omega)=\frac{\tau E_0}{2\sqrt{\pi}}e^{-\tau^2(\omega-\omega_c)^2/4}, \tag{31}$$

where ω_c is the carrier frequency of the pulse. By defining

$$\xi = \omega - \omega_c \tag{32}$$

and $\phi_1(z,t)$ through

$$\psi_1(z,t) = E_0 \phi_1(z,t) e^{-i\omega_c t}, \tag{33}$$

we can find $\phi_1(z,t)$ from Eq. (27):

$$\phi_1(z,t) = \frac{\tau}{2\sqrt{\pi}} \int e^{-\tau^2 \xi^2/4} \{[1 + r(\xi+\omega_c)] Q_{11}(z,\xi+\omega_c) \tag{34}$$

$$+ i[1 - r(\xi+\omega_c)] Q_{12}(z,\xi+\omega_c)\} e^{-i\xi t} d\xi, \tag{35}$$

which is the dimensionless slowly varying envelope of the electric component $\psi_1(z,t)$. The dimensionless slowly varying envelope of the magnetic component $\psi_2(z,t)$ is defined through

$$\psi_2(z,t) = E_0 \phi_2(z,t) e^{-i\omega_c t}. \tag{36}$$

From Eq. (28), we find

$$\phi_2(z,t) = \frac{\tau}{2\sqrt{\pi}} \int e^{-\tau^2 \xi^2/4} \{[1 + r(\xi+\omega_c)] Q_{21}(z,\xi+\omega_c) \tag{37}$$

$$+ i[1 - r(\xi+\omega_c)] Q_{22}(z,\xi+\omega_c)\} e^{-i\xi t} d\xi. \tag{38}$$

The dimensionless slowly varying envelope of electric displacement is written as

$$\phi_3(z,t) = \frac{\tau}{2\sqrt{\pi}} \int \epsilon(\omega) e^{-\tau^2 \xi^2/4} \{[1 + r(\xi+\omega_c)] \times Q_{11}(z,\xi+\omega_c) \tag{39}$$

$$+ i[1 - r(\xi+\omega_c)] Q_{12}(z,\xi+\omega_c)\} e^{-i\xi t} d\xi. \tag{40}$$

The energy density for nonmagnetic materials is

$$U(z,t) = \epsilon_0 |E_0|^2 u(z,t), \tag{41}$$

where the dimensionless energy density

$$u(z,t) = \frac{1}{4} \{\mathrm{Re}[\phi_1(z,t)\phi_3^*(z,t)] + \mathrm{Re}[\phi_2(z,t)\phi_2^*(z,t)]\}. \tag{42}$$

The Poynting vector can be expressed as

$$S(z,t) = c\epsilon_0 |E_0|^2 s(z,t), \tag{43}$$

where the dimensionless Poynting vector

$$s(z,t) = \frac{1}{2} \mathrm{Re}[i\phi_1(z,t)\phi_2^*(z,t)]. \tag{44}$$

A. Quarter stack of constant refractive indexes

We first consider a quarter wave stack where all layers are characterized by two constant refractive indexes. The parameters of the 1DPC is chosen as the same as those used by Steinberg *et al.* [2]. The 1DPC has a structure of $(AB)^5A$ with the refractive indexes $n_A = 2.22$ and $n_B = 1.41$. The optical thickness of each layer is $n_A d_A = n_B d_B = \lambda_0/4$, where $\lambda_0 = 692$ nm is the midgap wavelength. The midgap frequency is $\omega_0 = 2\pi c/\lambda_0$ and the corresponding optical period is $\tau_0 = 2\pi/\omega_0$. The total thickness of the sample is about 1081 nm. When light through the same vacuum distance as the sample thickness, it takes a time of 3.6 fs.

Suppose the carrier frequency of the Gaussian pulse is $\omega_c = \omega_0$, and the characterized time of the pulse is $\tau = 30\tau_0$. In Fig. 1(a) and (b) we show the temporal-spatial evolution behaviors of the dimensionless slowly varying envelopes $|\phi_1(z,t)|$ and $|\phi_2(z,t)|$, respectively. The time origin is take as the instant at which the peak of the incident Gaussian pulse arrives at the surface of $z = 0$. It is shown that at any spatial position, the temporal profiles of both electric field $|\phi_1(z,t)|$ and magnetic field $|\phi_2(z,t)|$ are approximately a Gaussian curve. Although the attenuated tendency from the incident end to the exit end for $|\phi_1(z,t)|$ and $|\phi_2(z,t)|$ is the same, the details of them are quit different. The node positions of $|\phi_1(z,t)|$ are the antinode positions of $|\phi_2(z,t)|$.

From the temporal-spatial curves we are able to find out the time at which the electric field or magnetic field reaches its maximum at any position. The times corresponding to the maximum $|\phi_1(z,t)|$ and the maximum $|\phi_2(z,t)|$ at different positions are shown in Fig. 2. In the first half part of the 1DPC, the field at the node position reaches the peak at about $t = -16.6$ fs. While at most other positions, the field reaches the maximum in an interval of time from 0.7 fs to 1.7 fs. Since the electric field and the magnetic field are not in phase, we cannot define the time delay by the peak of $|\phi_1(z,t)|$ or by the peak of $|\phi_2(z,t)|$. The time delay should be defined by the peak of the density of energy. According to the definition of the density of energy, it depends on both electric field and magnetic field. Therefore, it should be calculated by Eq. (42). After calculating the density of energy we are able to find out the time t_M at which the density of energy reaches the maximum. Suppose the density of energy at the position z reaches the maximum at time t_M, the time delay can be determined by $t_d = t_M - t_0$, where t_0 is the time through the same vacuum distance. In Fig. 3 we plot the time delay. It is shown that the time delay become negative when $z > 200$ nm. The maximum negative delay $t_d = -2.1$ fs occurs in the interior of the 1DPC. At the exit end, the time delay is $t_d = -1.9$ fs. The time delay at the exit end is in agreement with the stationary-phase prediction [11], but it differs slightly from the experimental measurement of $-(1.47 \pm 0.21)$ fs [2].

If we use the peak time t_M to define the peak propagation velocity $v_M = z/t_M$, then we find that the maximum v_M is $3.4c$, as shown in Fig. 4 (see the triangles). The maximum v_M occurs in the interior, not at the exit end. In general, the peak propagation velocity in homogeneous media is equal to the group velocity that is defined by $d\omega(k)/dk$. However, in the case of finite 1DPCs, the peak propagation velocity v_M cannot be determined by an overall dispersion relation $\omega(k)$. The appearance of the peak is a result of coherent superpo-

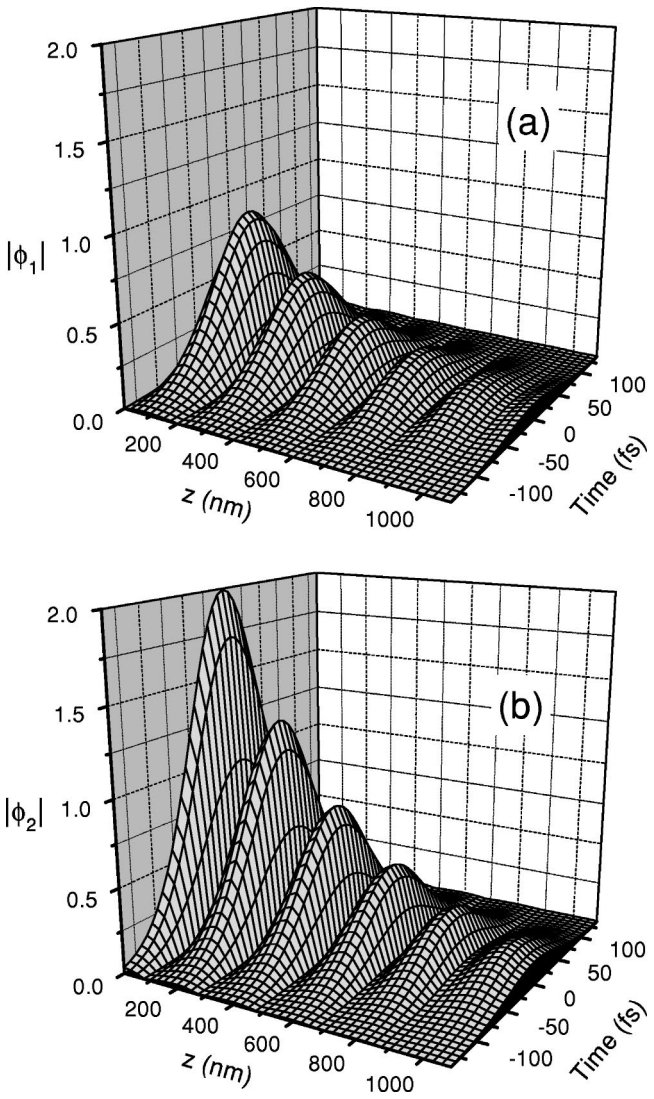

FIG. 1. The temporal-spatial evolution behaviors of the dimensionless slowly varying envelopes. (a) The electric component $|\phi_1(z,t)|$; (b) The magnetic component $|\phi_2(z,t)|$.

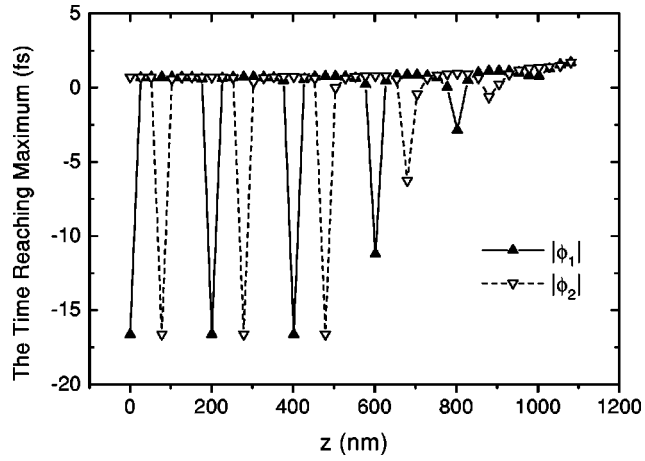

FIG. 2. The time at which the electric field (up triangle) or the magnetic field (down triangle) reaches the maximum.

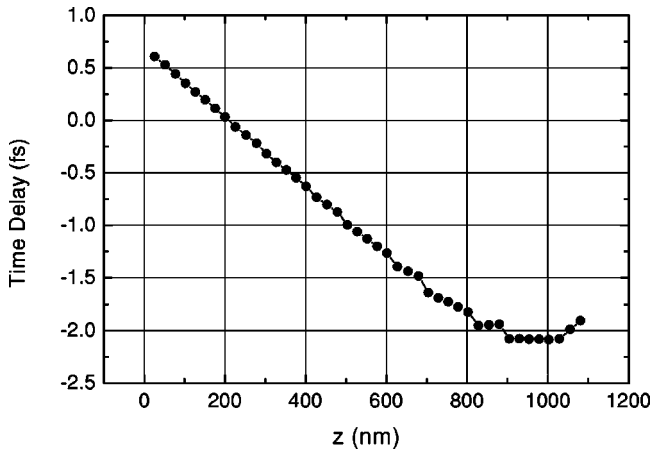

FIG. 3. The time delay inside the perfect quarter stack.

sition of forward waves and backward waves of all Fourier frequency components. It is the wave interference inside the 1DPC that leads to the reshaping of the Gaussian pulse. Since the evolution of the pulse in the 1DPCs is a reshaping processes, the peak velocity v_M cannot be understood as an ordinary group velocity.

The energy velocity v_E should be defined by the density of energy and the Poynting vector $v_E(z,t) = [s(z,t)/u(z,t)]c$. It is found that v_E is quite different from v_M. In Fig. 4, we plot the energy velocity v_E at the time when the density of energy reaches its maximum (see the squares). From our calculation we find that the maximum v_E is equal to $0.49\,c$. At any position and at any time the energy velocity never exceeds the light speed in vacuum c.

B. Quarter stack with a dispersive defect layer

Now we consider the case that a quarter-wave layer at the center is replaced by a half-wave layer. The structure of the 1DPC changes to *ABABADABABA*, where *D* is a half-wave defect with $n_D d_D = \lambda_0/2$ and $n_D = n_B$.

It is known that if a defect layer is placed into the 1DPC, a defect mode will appear in the stop band. At the defect

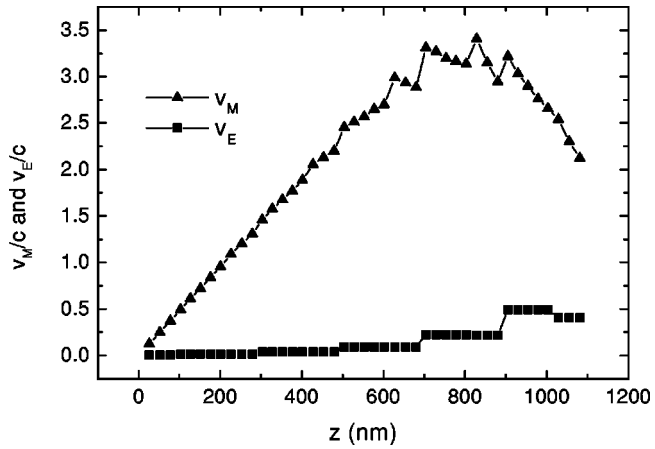

FIG. 4. The peak velocity $v_M = z/t_M$ and the energy velocity $v_E = S/U$, where U is the density of energy and S is the Poynting vector.

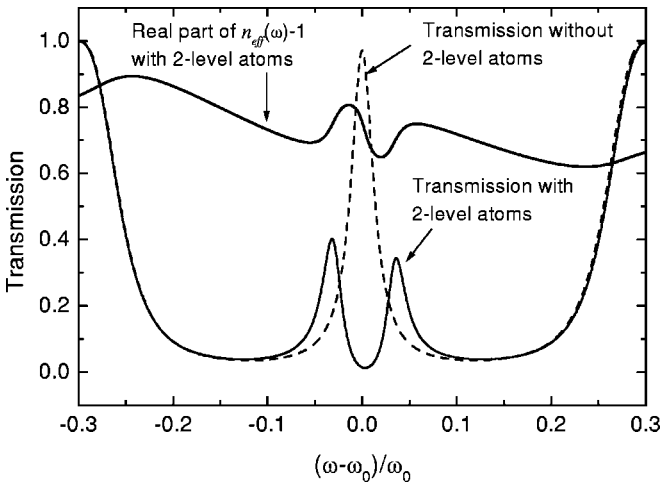

FIG. 5. The transmission through an 1DPC with a half-wave defect layer in the middle. Dashed line, the defect layer is nondisperive (without doped two-level atoms); thin solid line, the defect layer is doped with two-level atoms; heavy solid line, the real part of the effective refractive index.

mode frequency we can see a resonant transmission peak. The transmission peak is analogous to the narrow transmission peak in a complete absorption background of an electromagnetically induced transparency gas system, which leads to a steep dispersion curve with positive slope and causes to an extremely slow group velocity [15]. A calculation of effective refractive index showed that the resonant transmission peak in the band gap of 1DPC can as well produce a steep dispersion of the effective refractive index [6]. At the defect mode frequency the group delay is positive and extremely large. In Fig. 5 we show the transmission peak in the band gap by a dashed line for the 1DPC perturbed by a nondispersive half-wave defect layer.

The behavior of resonant transmission at band gap will be changed if two-level atoms are doped into the defect layer. We assume the linear susceptibility produced by the doped two-level atoms can be written as

$$\chi(\omega)=-\frac{\Gamma}{\omega-\omega_0+i\gamma}, \tag{45}$$

where Γ is proportional to the oscillator strength depending on the transition dipole moment and the density of the two-level atoms, and γ is the phenomenological linewidth. The transition frequency is assumed to be equal to the midgap frequency so that the Bragg resonance of the multilayerd structure is strongly coupled with the atomic resonance. The resultant dielectric function of the doped layer is

$$\epsilon(\omega)=\epsilon_B+\chi(\omega), \tag{46}$$

which contains a nonresonant background contribution $\epsilon_B=n_B^2$ in addition to the contribution of the dipole oscillators. The thin solid line in Fig. 5 indicates the transmission for the case with doped two-level atoms, where the linewidth is taken as $\gamma=0.01\omega_0$, and the oscillator strength is chosen such that $\Gamma=0.01\omega_0$. The single peak is split into a double peaks due to the two-level atoms. The minimum transmission is approximately equal to 0.012, which is approximately equal to the transmission of the perfect quarter stack. We find that the double peaks are analogous to the case of the double gain peaks of the three-level atoms used by Wang *et al.* who got a gain-assisted superluminal (negative) group velocity [16].

In finite 1DPCs, the group delay through the whole structure can be written as $t_d=t_0(n_g-1)$, where $n_g\equiv c/v_g$ is referred as to the group index. The group index can be determined by

$$n_g(\omega)=n(\omega)+\omega\frac{dn(\omega)}{d\omega}, \tag{47}$$

where $n(\omega)$ is the real part of an effective refractive index $n_{eff}(\omega)=n(\omega)+i\kappa(\omega)$ which is defined by the transmission coefficient $t=\sqrt{T}e^{i\phi}$. The real part of $n_{eff}(\omega)$ is [6,7]

$$n(\omega)=\frac{c\phi(\omega)}{L\omega}, \tag{48}$$

and its imaginary part is

$$\kappa(\omega)=-\frac{c}{2L\omega}\ln T(\omega), \tag{49}$$

where L is the total thickness. In Fig. 5 we plot the real part $n(\omega)$ of the effective refractive index with the heavy solid line. The dispersion of effective refractive index between the transmission peaks is anomalous, as the case between the gain peaks of the three-level in Ref. [16]. It is expected that similar superluminal propagation will occur in the 1DPC doped with the two-level atoms.

We first compare the temporal-spatial evolution of the fields for the cases with and without the doped two-level atoms. The characterized time of the Gaussian pulse is taken as $\tau=100\tau_0$ so that the pulse has a narrow spectrum band. In Fig. 6 we show the temporal-spatial behavior of $|\phi_1(z,t)|$ and $|\phi_2(z,t)|$ for the case without the doped atoms. In this case the energy is centered around the defect layer.

The defect layer becomes dispersive and absorptive when it is doped with two-level atoms. Due to the dispersion and absorption in the defect layer, the evolution of the fields is changed. The temporal-spatial evolutions of electric field $|\phi_1(z,t)|$, magnetic field $|\phi_2(z,t)|$, and electric displacement $|\phi_3(z,t)|$ are shown in Figs. 7(a), 7(b), and 7(c), respectively. The fields are no longer centered around the defect layer. They become attenuated fields, as the case in perfect quarter stack.

The effects of the two-level atoms on the time delay are shown in Fig. 8. In the case that no two-level atoms exist, the pulse propagation is subluminal with a large positive time delay. The maximum delay $t_d=23.8$ fs occurs at about $z=500$ nm, and the time delay at the exit end is $t_d=22.5$ fs. When the two-level atoms are doped, the subluminal propagation changes to superluminal propagation with large negative time delay. The negative delay can reach $t_d=-30.5$ fs at the exit end, which is much larger than the

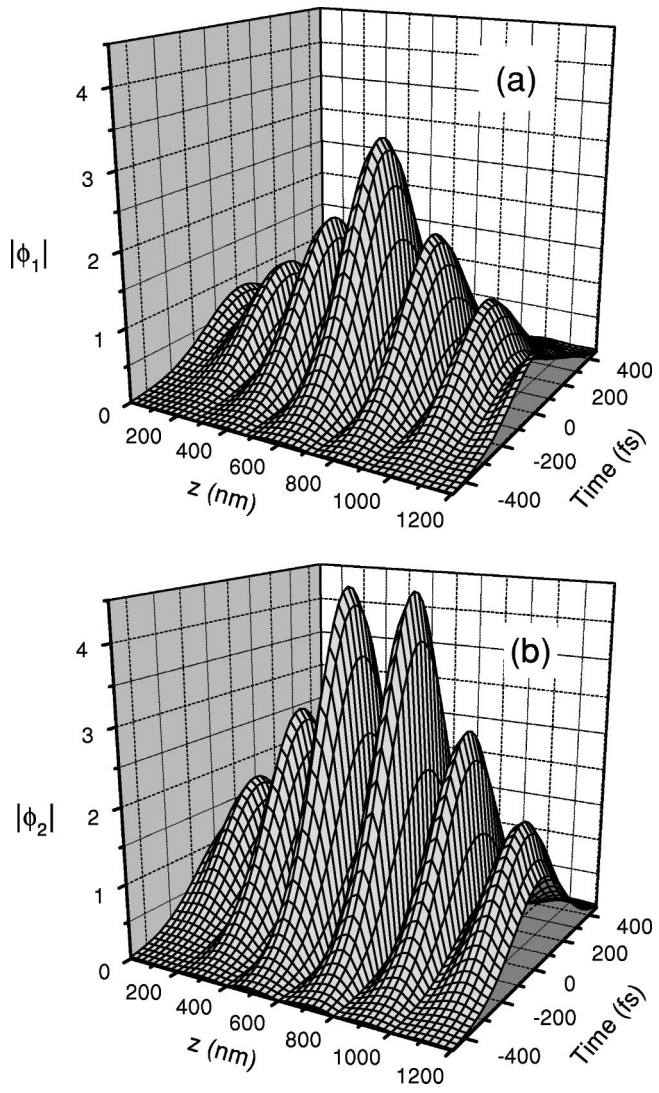

FIG. 6. The temporal-spatial evolution behaviors of the fields for the case that the defect layer is nondisperive (without doped two-level atoms): (a) The electric field $|\phi_1(z,t)|$; (b) The magnetic field $|\phi_2(z,t)|$.

delay $t_d=-1.9$ fs of perfect quarter stack. In the case of large negative time delay, the peak appears at the exit end before the incident peak reaches the input end, that is to say, it corresponds to a negative group velocity if we consider the thickness of the sample divided by the time when the peak appears at the exit end as the group velocity.

Although the peak of energy density appears before the arrival of the pulse peak through vacuum, the energy velocity never exceeds the light speed in vacuum. In Fig. 9 we show the energy velocity as function of z at the time when the energy density reaches its peak for the cases with and without the two-level atoms. The maximum v_E is approximately equal to $0.67c$. In the region behind the defect layer ($z>724$ nm), the energy velocities are the same for both cases. The minimum energy velocity is as slow as $0.09c$.

IV. CONCLUSIONS

We have investigated the temporal-spatial evolution of the pulse propagation in the 1DPC. The time delay is determined

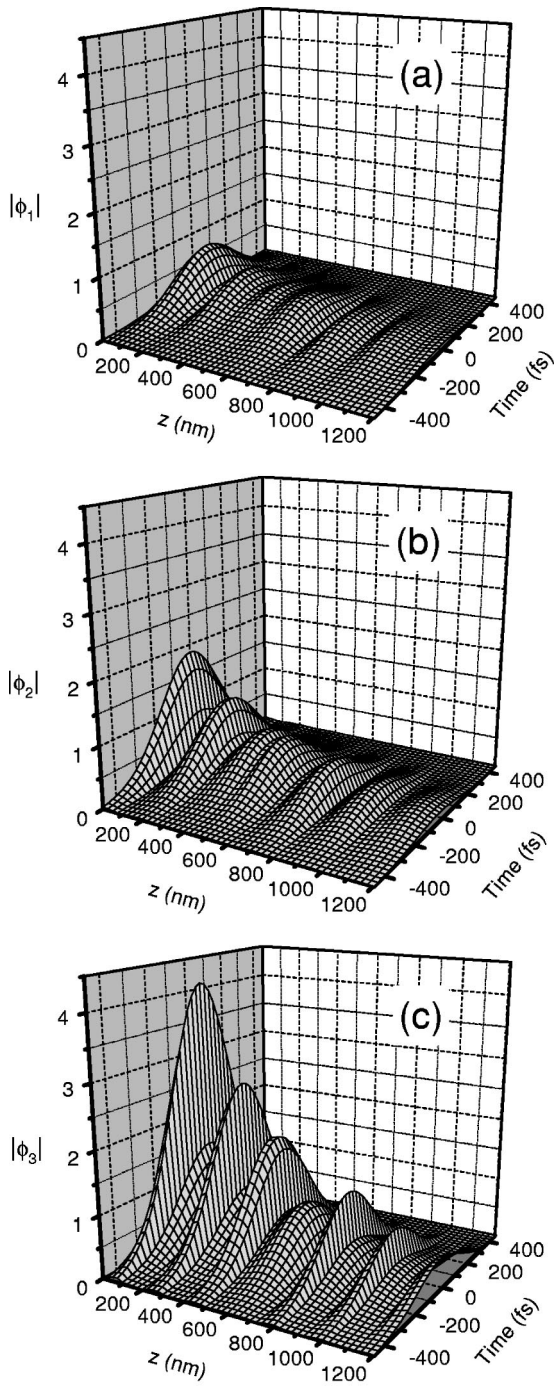

FIG. 7. The temporal-spatial evolution behaviors of the fields for the case that the defect layer is doped with two-level atoms: (a) The electric field $|\phi_1(z,t)|$; (b) The magnetic field $|\phi_2(z,t)|$; (c) The electric displacement $|\phi_3(z,t)|$.

by the peak time at which the density of energy reaches the maximum. The time delay at the exit end is agreement with the predication of stationary-phase method. In the stop band, the propagation through perfect quarter-stack is superluminal. The superluminal propagation changes to subluminal propagation if a nondispersive half-wave defect layer is placed into the periodic structure. If the half-wave defect layer is doped with two-level atoms such that the layer be-

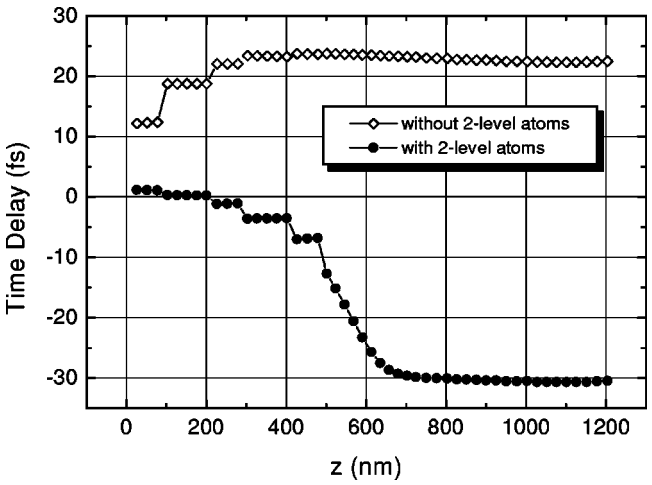

FIG. 8. The time delay for the case that the defect layer is nondisperive (open diamond) and for the case that the defect layer is doped with two-level atoms (solid circle).

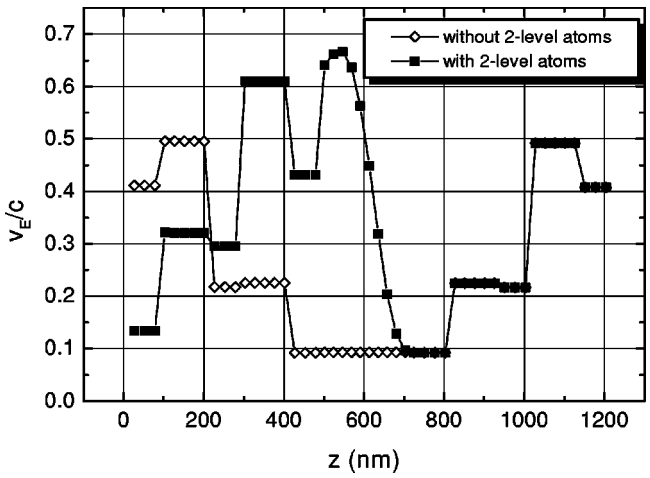

FIG. 9. The energy velocity for the case that the defect layer is nondisperive (open diamond) and for the case that the defect layer is doped with two-level atoms (solid square).

comes dispersive and absorptive, the subluminal propagation changes again to superluminal propagation with large negative time delay. The occurrence of the large negative time delay is a result of the Bragg resonance coupled with the atomic resonance.

We emphasize that the appearance of the pulse peak in the 1DPC before the pulse peak through the same vacuum distance is a result of the coherent superposition of the forward and backward waves for all Fourier frequency components with complicated relations of phases. It is a phenomenon of wave interference. Due to the interference, the pulse is reshaped inside the 1DPC. The peak velocity dose not represent the velocity of energy propagation. The energy velocity never exceeds the light speed in vacuum.

ACKNOWLEDGMENTS

This work was partly supported by FRG from HKBU and RGC from the HK Government, by the Foundation for University Key Teacher from the Ministry of Education of China, by the Foundation of 863 Project from National High-Tech ICF Committee in China, and by the National Natural Science Foundation from China under Contract No. 19947005.

[1] *Photonic Band Gaps and Localization*, edited by C.M. Soukoulis (Plenum, New York, 1993).
[2] A.M. Steinberg, P.G. Kwiat, and R.Y. Chiao, Phys. Rev. Lett. **71**, 708 (1993).
[3] Ch. Spielmann, R. Szipöcs, A. Stingl, and F. Krausz, Phys. Rev. Lett. **73**, 2308 (1994).
[4] A.M. Steinberg and R.Y. Chiao, Phys. Rev. A **51**, 3525 (1995).
[5] Amnon Yariv and Pochi Yeh, *Optical Waves in Crystals* (Wiley, New York, 1984), Chap. 6; Pochi Yeh, Amnon Yariv, and Chi-Shain Hong, J. Opt. Soc. Am. **67**, 423 (1977).
[6] S.Y. Zhu, N.H. Liu, H. Chen, and H. Zheng, Opt. Commun. **174**, 139 (2000).
[7] M. Centini, C. Sibilia, M. Scalora, G. D'Aguanno, M. Bertolotti, M.J. Bloemer, C.M. Bowden, and I. Nefedov, Phys. Rev. E **60**, 4891 (1999).
[8] M. Scalora, R.J. Flynn, S.B. Reinhardt, R.L. Fork, M.J. Bloemer, M.D. Tocci, C.M. Bowden, H.S. Ledbetter, J.M. Bendickson, J.P. Dowling, and R.P. Leavitt, Phys. Rev. E **54**, R1078 (1996).
[9] J.M. Bendickson, J.P. Dowling, and M. Scalora, Phys. Rev. E **53**, 4107 (1996).
[10] R.Y. Chiao and J. Boyce, Phys. Rev. Lett. **73**, 3383 (1994); A.M. Steinberg and R.Y. Chiao, Phys. Rev. A **49**, 2071 (1994); **49**, 3283 (1994); E.L. Bolda, J.C. Garrison, and R.Y. Chiao, *ibid.* **49**, 2938 (1994).
[11] R.Y. Chiao and A.M. Steinberg, *Progress in Optics XXXVII*, edited by E. Wolf (Elsevier, New York, 1997).
[12] Y. Japha and G. Kurizki, Phys. Rev. A **53**, 586 (1996).
[13] M. Scalora, J.P. Dowling, A.S. Manka, C.M. Bowden, and J.W. Haus, Phys. Rev. A **52**, 726 (1995).
[14] G. D'Aguanno, M. Centini, M. Scalora, C. Sibilia, M.J. Bloemer, C.M. Bowden, J.W. Haus, and M. Bertolotti, Phys. Rev. E **63**, 036610 (2001).
[15] L.V. Hau, S.E. Harris, Z. Dutton, and C.H. Behroozi, Nature (London) **397**, 594 (1999).
[16] L.J. Wang, A. Kuzmich, and A. Dogariu, Nature (London) **406**, 277 (2000).